CHAPTER 28

Multidomain Spectral Solution of Shock-Turbulence Interactions

David A. Kopriva*
M. Yousuff Hussaini†

Abstract. The use of a fitted-shock multidomain spectral method for solving the time dependent Euler equations of gasdynamics is described. The multidomain method allows short spatial scale features near the shock to be resolved throughout the calculation. Examples presented are of a shock- plane wave, shock-hot spot and shock-vortex street interaction.

1. Introduction. Spectral methods are global approximation methods in which solution unknowns are expanded in polynomials which are the eigenfunctions of a singular Sturm-Liouville problem. The primary advantage of these expansions is the rapid rate of convergence for problems with smooth solutions. However, the global nature of the approximation can also be a drawback. In particular, it is difficult to handle complicated geometries and to resolve locally important features.

Domain decomposition is one way to avoid the disadvantages of global approximation functions. The need for global mappings is eliminated when a computational domain is broken down into several smaller subdomains. It also be-

* Mathematics Department and Supercomputer Computations Research Institute Florida State University, Tallahassee, FL 32306. This research was supported in part by the Florida State University through time granted on its Cyber 205 supercomputer.

† Institute for Computer Applications in Science and Engineering(ICASE), NASA Langley Research Center, Hampton, VA 23665. Research was supported by the National Aeronautics and Space Administration under NASA Contract No. NAS1-18107 while in residence at ICASE.

comes easy to resolve important features of a solution since expansions of different orders can be used in different subdomains. The use of multidomain spectral methods for these purposes can be found, for example, in the papers by Kopriva [4,5].

In this paper, we use domain decomposition and grid refinement to resolve short spatial scale phenomena which are generated during a shock-plane wave, a shock-hot spot, and a shock-vortex street interaction in two spatial dimensions. For the shock-plane wave problem, we use Chebyshev- Fourier collocation within each subdomain. For the other problems, Chebyshev-Chebyshev collocation is used.

2. Shock Interaction Problem. We assume that the initial state of each shock interaction problem is a uniform gas, rapidly moving from left to right, which terminates in an infinite, normal shock. To the right of the shock, the gas is quiescent except for some specified fluctuation. This fluctuation might be a pressure, vorticity or entropy perturbation (or any combination of the three). As time progresses, the shock moves to the right and passes through the fluctuation. A result of this interaction is that the strength of the perturbation may be amplified or damped. A wave of one given type may also generate travelling waves of the other two types. The important feature of these waves from a numerical point of view is that while entropy and vorticity fluctuations move with the gas, sound waves move at the sound speed relative to the speed of the gas. This means that, spatially, there are two length scales associated with features generated by the shock: one corresponds to acoustic responses which will move far from the shock, the other is associated with entropy and vorticity responses which remain near the shock. A detailed discussion of the shock-turbulence interaction problem can be found in Zang, Hussaini and Bushnell [9].

The shock is handled by fitting it as a moving boundary. In the streamwise (x) direction the computational domain consists of the continually expanding region between the moving shock and a fixed upstream boundary at which inflow boundary conditions can be applied. In the computational domain, we model the gas by the inviscid Euler gas-dynamics equations. Because the shock is fitted, it is appropriate to write the equations in non-conservation form in terms of the logarithm of the pressure (P), velocity (u,v) , entropy (s) and temperature (T)

$$\begin{aligned} P_t + uP_x + vP_y + \gamma(u_x + v_y) &= 0 \\ u_t + uu_x + vv_y + TP_x &= 0 \\ v_t + uv_x + vv_y + TP_y &= 0 \\ s_t + us_x + vs_y &= 0 \end{aligned} \tag{1}$$

For the ratio of specific heats, γ, a value of 1.4 is used.

Previous numerical simulations of shock-turbulence interactions have included finite difference calculations by Zang, Hussaini and Bushnell [9]. Pao

and Salas [6] also used a finite difference method to compute the related problem of the generation of sound waves by a shock-vortex interaction. Single-domain spectral solutions to the shock-turbulence and shock-vortex interactions were reported by Salas, Zang and Hussaini [7], Zang, Kopriva and Hussaini [8] and Hussaini, Kopriva, Salas and Zang [3]. In each case, the use of the expanding computational domain meant that the effective resolution of the grid and the accuracy of the solution decreased as the calculation progressed in time.

3. Multidomain Strategy. Figure 1 illustrates the use of domain decomposition to allow for grid refinement near the shock when the moving shock is fitted. The region between the fixed inflow boundary and the moving shock boundary is divided into a number of strips (subdomains). The interface positions are constant in the vertical direction, but vary in time to allow them to move with the shock. In this way, constant grid resolution can be maintained near the shock where the short scale effects of the interaction occur.

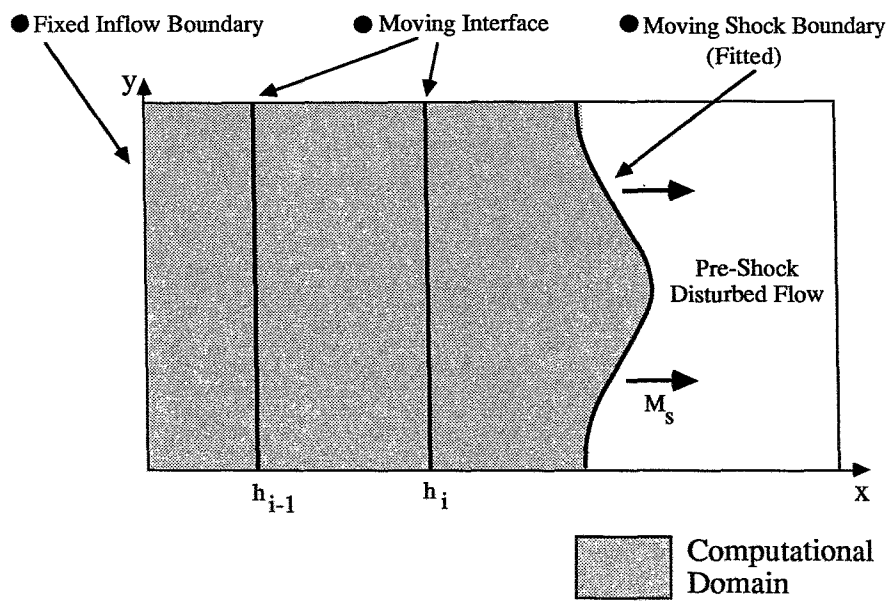

Figure 1. Diagram of the computational domain for the shock-turbulence interaction

Because the flow to the right of the shock is completely determined by a specified perturbation of a quiescent gas, we compute within a semi-infinite region between the shock and an arbitrarily placed upstream boundary $x = h_0$. For notational purposes, we will denote the shock position by $h_K(y,t)$. The

extent of the region in the vertical direction is $-\infty < y < \infty$. We subdivide the region between the shock and the inflow boundary into K strips by placing interfaces at positions $x = h_i(y,t)$, $i = 1,2,\ldots,K-1$. Each subdomain is then mapped onto a unit square. In the streamwise direction, we use the mapping

$$X = \frac{(x - h_{i-1}(y,t))}{(h_i(y,t) - h_{i-1}(y,t))} \tag{2}$$

The mapping in the vertical direction depends on whether the problem is periodic or non-periodic. The shock-plane wave interaction problem is periodic in the vertical direction. For that problem we use

$$Y = y/L \tag{3a}$$

where L is the vertical length scale. For the other problems, we use the mapping

$$Y = \frac{1}{2}\left(1 + \frac{y}{\sqrt{\alpha^2 + y^2}}\right) \tag{3b}$$

where α is a parameter which governs the clustering of the grid points near $y = 0$.

In the mapped coordinates on each subdomain, eq. 1 can be written as the system

$$Q_t + AQ_X + BQ_Y = 0 \tag{4}$$

where $Q = [P\ u\ v\ s]^T$. The coefficient matrices are

$$A = \begin{bmatrix} U & \gamma X_x & \gamma X_y & 0 \\ TX_x & U & 0 & 0 \\ TX_y & 0 & U & 0 \\ 0 & 0 & 0 & U \end{bmatrix} \quad \text{and} \quad B = \begin{bmatrix} V & \gamma Y_x & \gamma Y_y & 0 \\ TY_x & V & 0 & 0 \\ TY_y & 0 & V & 0 \\ 0 & 0 & 0 & V \end{bmatrix}$$

where the variables U and V represent the contravariant velocity components $U = X_t + uX_x + vX_y$ and $V = uY_x + vY_y$.

Within each subdomain, the solution, Q, is approximated by a grid function, Q_{ij}, at a finite number of collocation (grid) points (X_i, Y_j). In the X direction, the collocation points are the nodes of the Gauss-Lobatto-Chebyshev quadrature rule mapped onto [0,1]:

$$X_i = \frac{1}{2}(1 - \cos(i\pi/N)) \quad i = 0,1,\ldots,N \tag{5}$$

In the vertical direction, the uniform grid

$$Y_j = j/M \quad j = 0,1,\ldots,M \tag{6a}$$

is used for the plane wave interaction problem. For the others, the Gauss-Lobatto grid

$$Y_j = \frac{1}{2}(1 - \cos(j\pi/M)) \quad j = 0, 1, \ldots, M \tag{6b}$$

is used.

Each derivative of Q at the grid points is approximated by the corresponding derivative of the spectral interpolant which passes through the Q_{ij}'s. For problems which are periodic in the vertical direction, this interpolant is the Chebyshev-Fourier expansion

$$Q(X,Y,t) = \sum_{p=0,q=-M/2}^{N,M/2-1} \widetilde{Q}_{pq}(t) T_p(2X-1) e^{2\pi i q Y} \tag{7}$$

Problems which are periodic in neither direction require a Chebyshev-Chebyshev expansion

$$Q(X,Y,t) = \sum_{p=0,q=0}^{N,M} \widetilde{Q}_{pq}(t) T_p(2X-1) T_q(2Y-1) \tag{8}$$

For details, see Canuto, Hussaini, Quarteroni and Zang [1].

Five types of boundary conditions are required. At the far right is the shock boundary which is fitted in the manner described by Pao and Salas [6]: An ordinary differential equation is derived for the motion of the shock and this is integrated along with the interior equations. At the inflow boundary on the left, a characteristic boundary condition is used. If the inflow boundary is subsonic, the velocity and entropy are fixed in time. The pressure is computed by integrating the compatibility equation

$$P_t = (U - aX_x)\left(\frac{\gamma}{a} u_X - P_X\right) \tag{9}$$

which is derived from the pressure and momentum equations and is written in terms of the sound speed, $a = \sqrt{\gamma T}$. If the boundary is supersonic, all variables are fixed in time.

The boundaries at infinity for the non-periodic problems are actually boundaries at large values of y. There, the velocities and the entropy are computed from the interior approximation. The pressure is determined by extrapolating along a characteristic projection normal to the boundary in the manner described by Gottlieb, Gunzburger and Turkel [2]. Periodic boundary conditions are handled trivially by the Fourier approximation.

At an interface, the approximation to the X derivative uses a weighted average of the derivatives from the left and right sides. We write

$$Q_t + A^L Q_X^L + A^R Q_X^R + B Q_Y = 0 \tag{10}$$

where Q_X^L, Q_X^R are the spectral derivative approximations from the left and the right. Since the problem is hyperbolic, it is necessary that information is propagated in the proper directions. Thus, a characteristic weighting is necessary and the left and the right coefficient matrices are written as

$$A^L = 1/2(A + |A|), \quad A^R = 1/2(A - |A|)$$

The matrix absolute value is defined as

$$|A| = Z|\Lambda|Z^{-1}$$

where Z is the matrix of the right eigenvectors of A and Λ is the diagonal matrix of eigenvalues. For the problem solved here, the matrix absolute value at an interface is quite simply

$$|A| = \frac{1}{2}\begin{bmatrix} (\lambda^+ + \lambda^-) & \gamma/a(\lambda^+ - \lambda^-) & 0 & 0 \\ a/\gamma(\lambda^+ - \lambda^-) & (\lambda^+ + \lambda^-) & 0 & 0 \\ 0 & 0 & 2\lambda^0 & 0 \\ 0 & 0 & 0 & 2\lambda^0 \end{bmatrix} \tag{11}$$

where $\lambda^{\pm} = U \pm aX_x$ and $\lambda^0 = U$ are the eigenvalues of A.

3. Applications.

3.1 Shock-Plane Wave Interaction. The first application that we consider is the interaction of a Mach 8 supersonic shock with a plane pressure wave. Ahead of the shock, the pressure perturbation is given by

$$p' = \beta\epsilon^{i(\mathbf{k}\cdot\mathbf{x}-\omega t)} \tag{12}$$

where the vector $\mathbf{k} = k(\cos(\theta), \sin(\theta))$ is the wavenumber vector, ω is the frequency and β is the amplitude. The angle of incidence, θ, is measured normal to the shock. See Zang et. al [9] for a detailed description of this problem.

To avoid overshoots associated with an abrupt start of the wave, the amplitude, β, is multiplied by the factor

$$s(t) = \begin{cases} 3(t/t_s)^2 - 2(t/t_s)^3 & 0 \le t \le t_s \\ 1 & t \ge t_s \end{cases} \tag{13}$$

The startup time, t_s, is chosen as $1/2$ the time it takes the shock to encounter one full wavelength of the incident wave.

Linear theory predicts that the pressure wave will be amplified and diffracted by the shock. Also, a plane vorticity and entropy wave will be generated. We can define the pressure transmission coefficient as the ratio of the refracted to incident

pressure wave amplitudes. The vorticity or entropy transmission coefficients are the ratio of the generated wave amplitude to the incident pressure amplitude.

Fig. 2 shows the pressure and vorticity transmission coefficients at $t = 0.2$ for a 10% ($\beta = 0.1$) amplitude pressure wave incident at 30° to the shock. Three subdomains were used, each with 16 horizontal and 8 vertical grid points. At the time indicated, the interfaces were at $x = 0.7$ and $x = 1.5$. The transmission coefficients were computed at each grid line in x from the first coefficient of the Fourier transform of the solution in the vertical direction. Compared with the computed solutions are the predictions of the linear theory.

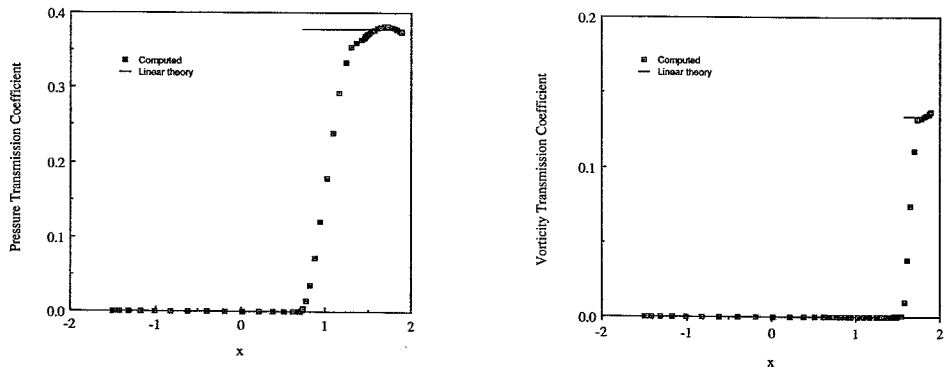

Figure 2. Dependence at $t = 0.21$ of acoustic (left) and vorticity (right) responses to an acoustic wave incident at 30° to a Mach 8 shock.

The computed responses clearly occur on two different length scales, the extent of the vorticity behind the shock being roughly one fourth that of the pressure. Nevertheless, it was possible to resolve the vorticity wave with eight grid points in the horizontal direction. This high resolution is necessary because the vorticity is computed from derivatives of the flow variables. Single domain

calculations show noisy transmission coefficient profiles for the vorticity [8,9].

3.2 Shock-Hot Spot Interaction. A physically more complex problem is the interaction of a shock with a temperature spot. In this case, the temperature ahead of the shock is prescribed by

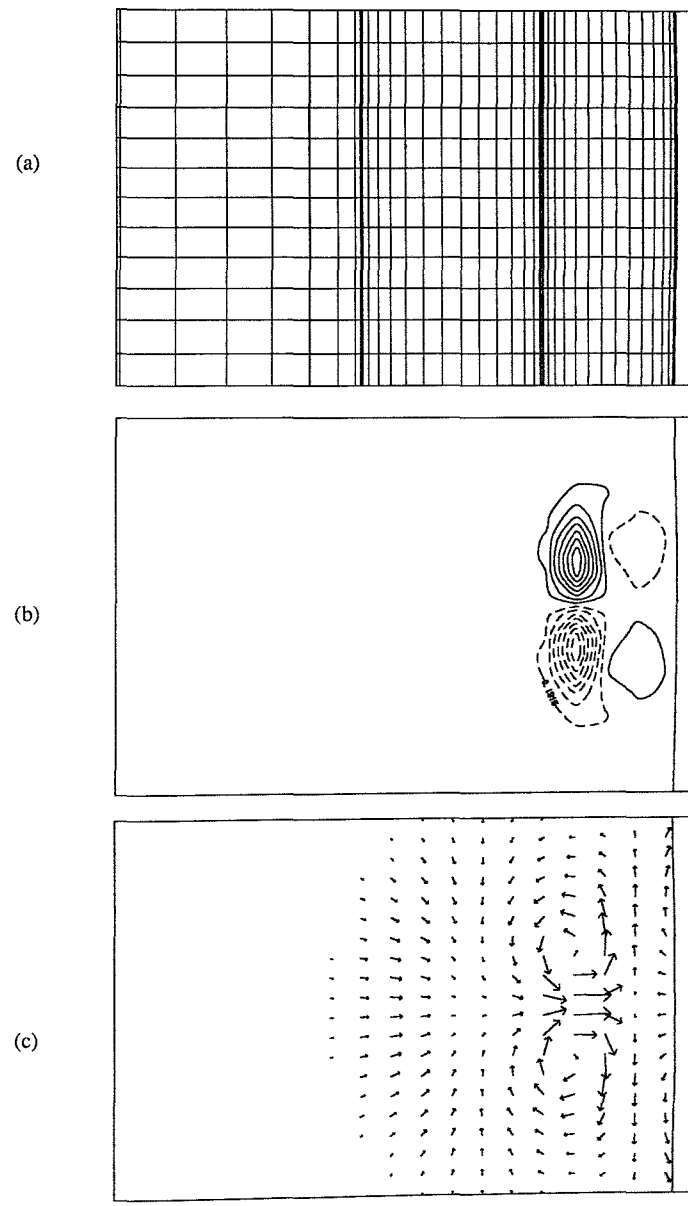

Figure 3. Grid (a), Vorticity contours (b) and velocity vectors (c) for the 25% hot spot interaction with a Mach 2 shock at time $t = 0.5$.

$$T(x,y) = 1 + \varepsilon\epsilon^{-\left[(x-x_o)^2+y^2\right]/2\sigma^2} \tag{14}$$

where ε is the maximum fractional temperature perturbation, $(x_o, 0)$ is the center of the spot and σ is its width. For this simulation, we chose $\varepsilon = 0.25$, $x_o = 0.5$, and $\sigma = 0.1$.

Figure 3 shows the grid, vorticity contours and velocity vectors at time, $t = 0.5$. Again, three subdomains were used, this time with 15 horizontal and 40 vertical grid points in each. What is actually shown are the results on a portion of the grid near the shock and hot spot covering the physical space rectangle $[-.25,\ 1.25] \times [-.5,\ .5]$. Notice the strong counter-rotating vortices which have been generated by the shock. A weaker set also appears to have been generated even closer to the shock.

3.3 Shock-Vortex Street Interaction. In this case, the initial perturbation ahead of the shock is a vortex field. The stream function for this field is

$$y = \frac{\kappa}{2\pi}\log\left[\cosh\left(\frac{2\pi}{c}\sqrt{r^2 + (y \pm b/2)^2} - \cos\left(\frac{2\pi}{c}(x \pm c/2)\right)\right)\right] \tag{15}$$

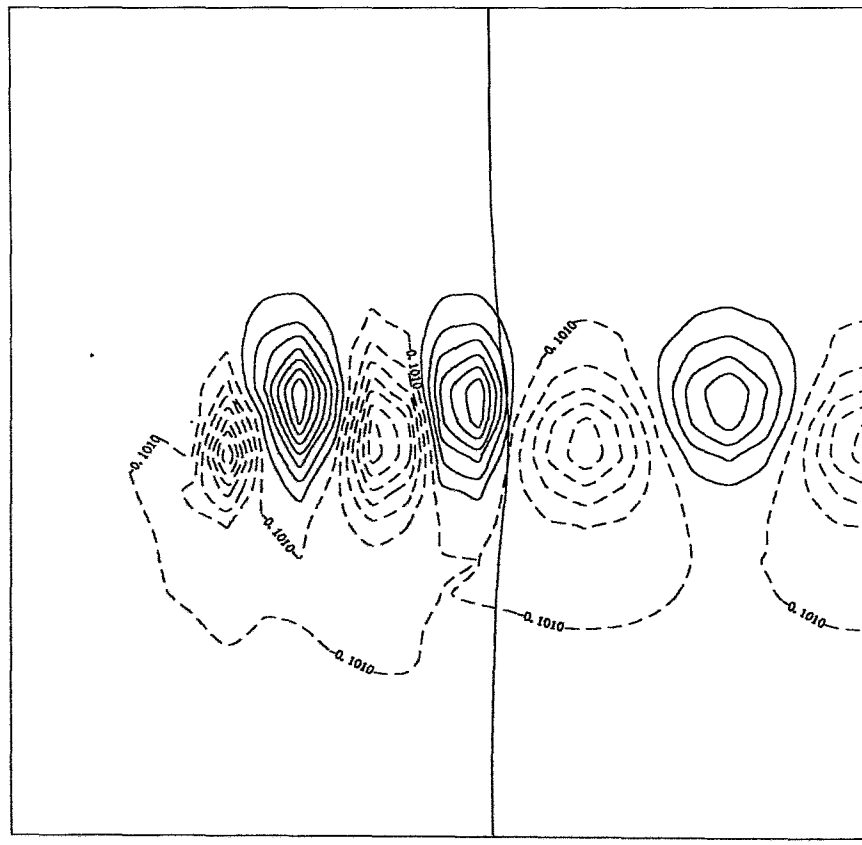

Figure 4. Vorticity contours at $t = 0.36$ for a Karman vortex street after interaction with a Mach 1.3 Shock.

The circulation, core radius, shock Mach number and vortex separation parameters used were $\kappa = 0.186$, $r = 0.1$, $M_s = 1.3$, $c = 0.33$ and $b = 0.048$ to correspond to the single domain calculation of Salas, Zang and Hussaini [7].

Figure 4 shows the vorticity contours of the shock-vortex street interaction at time, $t = 0.36$, for a three subdomain calculation. Within each subdomain a 15×40 grid was used. Notice the longitudinal compression and lateral elongation of the vortex field behind the shock. The results are also quite smooth. This is to be contrasted with the single domain calculations of [7] which required strong filtering every 160 time steps and still produced solutions which were not smooth. No artificial smoothing was required for this multidomain calculation.

4. Summary. The solution of three simple shock-turbulence interaction models has been described. Each problem has the characteristic that the length scales associated with the pressure and with the entropy/vorticity are substantially different, thus making it difficult to resolve them efficiently in the horizontal direction with a single Chebyshev grid. By using domain decomposition it was possible to resolve these two length scales.

REFERENCES

(1) C. Canuto, M. Y. Hussaini, A. Quarteroni and T. A. Zang, *Spectral Methods in Fluid Dynamics*, Springer-Verlag, New York, 1987.

(2) D. Gottlieb, M. Gunzburger and E. Turkel, *On Numerical Boundary Treatment of Hyperbolic Systems for Finite Difference and Finite Element Methods*, SIAM J. Numer. Anal., **19** (1982), pp. 671–682.

(3) M. Y. Hussaini, D. A. Kopriva, M. D. Salas,and T. A. Zang, *Spectral Methods for the Euler Equations: Part II - Chebyshev Methods and Shock Fitting*, AIAA Journal, **23** (1985) pp. 234–240.

(4) D. A. Kopriva, *A Spectral Multidomain Method for the Solution of Hyperbolic Systems*, Applied Numerical Math., **2** (1986), pp. 221–241.

(5) D. A. Kopriva, *Solution of Hyperbolic Equations on Complicated Domains with Patched and Overset Chebyshev Grids*, FSU-SCRI-87-35 preprint. Submitted to SIAM J. Sci. Stat. Comp.

(6) S. P. Pao and M. D. Salas, *A Numerical Study of Two-Dimensional Shock Vortex Interaction*, AIAA Paper 81-1205, 1981.

(7) M. D. Salas, T. A. Zang and M. Y. Hussaini, *Shock Fitted Euler Solutions to Shock-Vortex Interactions*, Proceedings of the 8th International Conference on Numerical Methods in Fluid Dynamics, E. Krause, ed., Springer-Verlag, New York, 1982, pp. 461–467.

(8) T. A. Zang, D. A. Kopriva and M. Y. Hussaini, *Pseudospectral Calculation of Shock Turbulence Interactions*, Proceedings of the 3rd International Conference on Numerical Methods in Laminar and Turbulent Flow, C. Taylor, ed., Pineridge Press, Swansea, Wales, 1983, pp. 210–220.

(9) T. A. Zang, M. Y. Hussaini, and D. M. Bushnell, *Numerical Computations of Turbulence Amplification in Shock Wave Interactions*, AIAA Journal, **22** (1984), pp. 13–21.